POLYMERS FOR ADVANCED TECHNOLOGIES
Polym. Adv. Technol. **13**, 1032–1038 (2002)
Published online in Wiley InterScience (www.interscience.wiley.com). DOI:10.1002/pat.236

Healing of Adsorbed Polymer Layers in a Narrow Gap Following Removal by Shear†

Uri Raviv[1]* and Jacob Klein[1,2]

[1]*Department of Materials and Interfaces, Weizmann Institute of Science, Rehovot 76100, Israel*
[2]*Physical and Theoretical Chemistry Laboratory, Oxford University, South Parks Road, Oxford OX1 3QZ, UK*

ABSTRACT

The shear and normal forces between layers of poly-(ethylene oxide) (PEO), of molecular weights $M_w = 37$ kg/mol adsorbed onto smooth, curved solid (mica) surfaces across the good solvent toluene have been determined using a surface force balance (SFB). The equilibrium $F_n(D)$ profiles are closely similar to those measured in earlier studies between adsorbed PEO layers. The shearing motion causes the removal of polymer from within the intersurface gap during sliding. The recovery of the adsorbing layer has been measured and the amount of adsorption with time was calculated. Our findings showed that there is no migration of polymers on the surfaces and that the recovery of the layer is controlled by the rate of diffusion of polymer chains into the gap. Copyright © 2003 John Wiley & Sons, Ltd.

KEYWORDS: adsorbed polymers; poly(ethylene oxide); surface forces; polymer diffusion; narrow gap

*Correspondence to: U. Raviv, Department of Materials and Interfaces, Weizmann Institute of Science, Rehovot 76100, Israel.
E-mail: uri.raviv@weizmann.ac.il
†This paper was presented at PAT 2001–Eilat, Israel.

INTRODUCTION

Interactions between surfaces bearing surface-attached polymer layers immersed in a liquid medium have direct implications for a wide range of technologies. These include colloidal stabilization and destabilization [1, 2], adhesion [3], thin-film stability [4–6], control of surface energies and biocompatibility [5], and protective (anti-fouling) surface coatings in filtration applications [7, 8]. Such forces have been measured, using a variety of methods, and are reasonably well understood [9]. The surface force balance (SFB) technique in particular has been used to characterize normal and shear forces between surfaces in a variety of systems [10–25].

Poly(ethylene oxide) (PEO) has been the subject of many studies. It is known for its low toxicity and biocompatibility with the immune system of the human body [26] and for its chemical inertness and its solubility both in organic and especially in aqueous solutions, in contrast to poly(methylene oxide) and to poly(propylene oxide) and higher analogues, none of which are water-soluble [27]. Direct measurements of the shear and normal forces between two atomically smooth mica surfaces bearing adsorbed layers of PEO in the good solvent toluene [25, 28] or in water [29–31] were reported. It was found that when the load and friction are high, low-molecular-weight (M_w) PEO is removed from the intersurface gap during shear.

Here we examine in detail the recovery of the adsorbed layer following its removal by the shearing motion.

EXPERIMENTAL

Method

The SFB technique and detailed experimental procedures have been described earlier [25, 32, 33]. The present force balance, incorporating in particular both normal and shear force measuring capabilities, is shown schematically in the inset to Fig. 1. To recall briefly: two half-silvered mica sheets (thickness *ca.* 2 μm and atomically smooth on both sides) are mounted opposite each other on an upper and a lower cylindrical lens in a crossed-cylinder configuration (equivalent to a sphere on a flat). White-light multiple beam interferometry reveals the distance D between them (to ±0.2–0.3 nm) and the geometry of the contact region (including the mean radius of curvature R = *ca.* 1 cm). Fine motion in both normal (D) and lateral (x) directions is provided by a sectored piezoelectric tube. The normal and shear forces F_n and F_s are determined directly from the bending ΔD and Δx respectively of the two orthogonal springs, as $F_n = K_n \Delta D$ and $F_s = K_s \Delta x$, where $K_n = 100$ N/m and $K_s = 70$ N/m are the respective spring constants.

Materials

The ethanol and toluene used for cleaning were supplied by Bio-Lab Inc. (Jerusalem) and were analytical grade. The toluene used for the measurements was hypersolvent grade for HPLC 99.8% (BDH Laboratory), and used as received. The mica was ruby muscovite, grade 1, supplied by S & J Trading Inc. (New York). The PEO used, terminated with a hydroxyl group and used as received, was supplied by Polymer Laboratories Ltd (UK). Its M_w is 37 kg/mol, $M_w/M_n = 1.07$, and its unperturbed gyration radius (R_g) is 6.2 nm. The molecular characteristics of the polymers used were determined by GPC and light-scattering (manufacturers' data).

Procedure

The surfaces are brought into contact in air to determines the $D = 0$ position. The surfaces are then separated (to *ca.* 2 mm) and the box is filled with toluene. After allowing 1 hour for thermal equilibration a normal force–distance profile, $F_n(D)$, is taken. PEO solution, in concentrations of 40 ± 5 μg/ml, was introduced by replacing the pure solvent with the polymer solution, while keeping a gap of 2 mm between the surfaces within which a liquid meniscus was maintained. Polymer was allowed to adsorb onto the surfaces for an incubation time of 12–16 hours (at 2 mm separation) following which $F_n(D)$ profiles were determined. Uniform back and forth shear motion was then applied to the top mica surface and the lateral force $F_s(D)$ between them was recorded over a range of surface separations D. $F_n(D)$ profiles were measured following shear measurements in order to check the effect of shear on the adsorbed layer and to study its recovery. The results described below are based on four separate experiments (different pairs of mica sheets).

RESULTS

Pure Toluene

In each experiment, prior to introducing the PEO solution, normal $F_n(D)$ profiles were measured between the bare mica surfaces immersed in pure toluene, to check for absence of contamination as noted. Results measured on both compression and decompression are shown in Fig. 1, where the force axis is normalized as $F_n(D)/R$: in the Derjaguin approximation (for $R \gg D$) $F_n(D)/2\pi R$ is the corresponding interaction energy $E(D)$ per unit area between two flat parallel surfaces, a distance D apart, obeying the same force–distance law [34].

This normalization enables comparison of $F_n(D)/R$ profiles from different experiments and is used in all subsequent normal and shear force profiles. No forces were detected for $D > 5$ nm below which the surfaces came into adhesive contact ($D = 1 \pm 1$ nm), in agreement with previous studies [28]. On separation the surfaces jump out (to a position where no forces are acting between them), owing to a mechanical instability expected

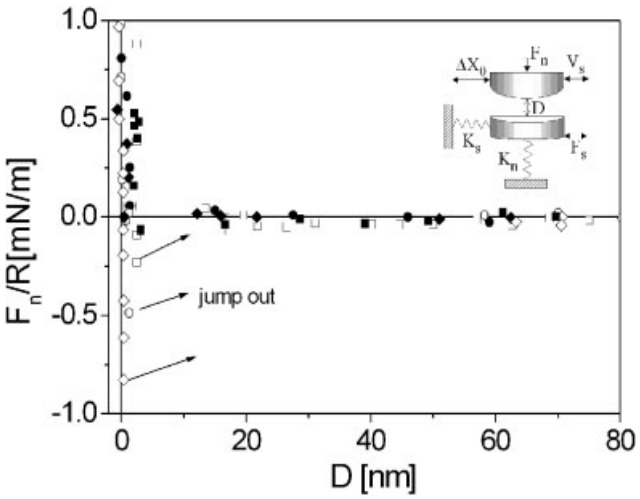

FIGURE 1. Normal force (F_n)–distance (D) profiles between curved mica surfaces in pure toluene, where the force axis is normalized as (F_n/R) (R = mean radius of curvature of the mica) to yield the interaction energy per unit area between flat parallel plates obeying the same $F_n(D)$ law, in the Derjaguin approximation [39]. Different symbols indicate different sets of experiments. Solid symbols are used for force profiles measured during compression of the two surfaces, while open symbols indicate force profiles measured during decompression. The inset shows schematically the main features of the SFB used [33], indicating the two orthogonal springs K_s and K_n whose bending measures directly the shear and normal forces F_s and F_n between the surfaces as the upper surface is moved laterally parallel ($\pm\Delta X_0$) or normal to the lower surface respectively.

whenever $\partial F_n(D)/\partial D > K_n$, the constant of the normal forces spring. The form of the interaction may be suggestive of some water condensation between the surfaces; we did not examine in detail the possible presence of structural forces [35], though the scatter of both repulsive and adhesive forces may indicate the presence of such effects. The main point is that the attraction indicated the absence of contaminants in the polymer-free system, while its range is small compared with the range of interactions once polymer had adsorbed. This simplifies subsequent interpretation of the results.

Normal and Shear Forces after the Addition of PEO

Following addition of the PEO solution at concentrations of 40 ± 5 μg/ml, the surfaces were allowed to incubate in the solution overnight at separation of 2 mm. Normal force profiles, shown in Fig. 2, were then determined prior to the shear measurements to ensure absence of contamination.

These profiles are very similar to those observed in earlier studies for the almost identical system of PEO (M_w = 40 kg/mol) adsorbed from toluene onto mica [28], which are shown for comparison, in Fig. 2 as solid lines (best fit to the results); the quantitative agreement is quite close. The main features are as follows: on initial compression a monotonic repulsion commences at a range of 7.3 ± 0.8 R_g, this defines the onset separation $D = 2L$, where L is the equilibrium thickness of the adsorbed layer. On decompression immediately following close approach, the forces are considerably shorter-ranged, probably indicating the forced adsorption of more segments onto the mica surface and a transient compressive distortion of the adsorbed layers. On subsequent recompression the layers relax back to their original (equilibrium) structure within 10 minutes following the first approach run (Fig. 2).

Shear forces between the compressed PEO-covered surfaces in the respective polymer solutions were measured by applying uniform back-and-forth shear motion, amplitude *ca.* 300 nm, at frequency 0.5 Hz, to the top surface, and monitoring the resultant bending of the shear spring on which the lower surface is mounted. Measurements were carried out, starting from the onset of normal repulsion and at decreasing separations, D, down to strong compressions. Figure 3 shows the shear forces F_s transmitted to the lower surface in response to the applied lateral back-and-forth motion Δx_0 of the top surface, as the surfaces approach to smaller separations, for the adsorbed PEO layers. The traces are reproduced directly from the XYt recorder.

Qualitatively, up to moderate compressions, no frictional forces are measurable above the noise level δF_s in the signal as the surfaces are compressed down to separations that are substantially smaller than $2L$. The initial regime where F_s becomes measurable is shown in Fig. 3A: shear

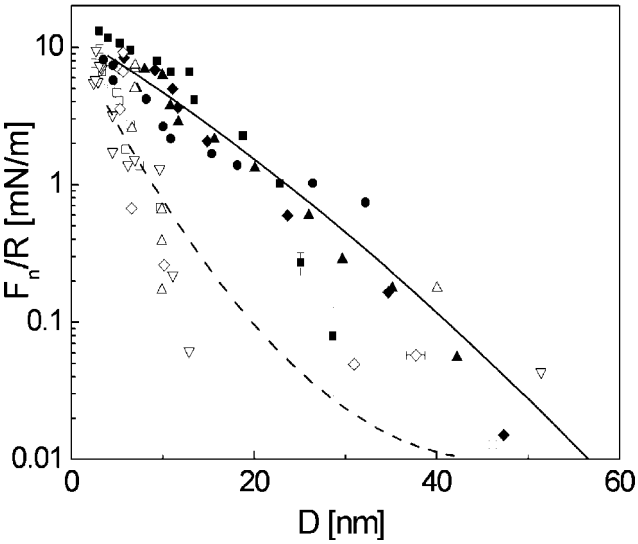

FIGURE 2. Normalized force-distance profiles (F_n/R) versus D following overnight incubation of the mica surfaces in 40 μg/ml solution of PEO in toluene. Measurements during compression and rapid decompression of the two surfaces are shown in different sets of experiments. Different symbols refer to different contact positions at different mica sheets. Solid symbols indicate forces measured during compression and open symbols indicate forces measured during decompression. We note that the profiles on a recompression immediately following a decompression are identical – within the scatter – to the original compression profile. The results are compared with curves summarizing the results of Luckham and Klein for PEO (M_w = 40 000) in similar conditions [28].

forces are first detected at compression ratios ($2L/D$) greater than about 4, that is at $D < 10$ nm. At higher compressions the shear forces transmitted to the lower surface, as the top surface moved back and forth, progressively increased.

The protocol for the shear force measurements is as follows. A normal compression–decompression run was carried out to ensure integrity of the layers just prior to the shear measurements. The surfaces were then enabled to approach slowly by thermal drift as the top surface moved laterally, while D was monitored simultaneously from the position of the interference fringes. As seen in Fig. 3, the initial response to shear is a rise in F_s (regions *a* or *c* in the shear traces), followed by a plateau region (*b* or *d* in the traces). In general, the applied lateral motion Δx_0 is related to the sliding between the surfaces, of extent $\Delta x_{sliding}$, and to the bending of the lower shear spring, of extent Δx, as $\Delta x_0 = \Delta x_{sliding} + \Delta x$ (we recall that the traces show $F_s = K_s \Delta x$). In the rise regions (*a* and *c* in the traces), $\Delta x_{sliding}$ represents the extent to which the opposing PEO layers slide past or disentangle from each other as the top surface rubs past the lower one; it is of order 80% of Δx_0 when F_s first becomes measurable (lower compressions), decreasing to *ca.* 20% of Δx_0 at the higher compressions. The extent of sliding increases towards the top of the rise region. At the top the shear force equals the

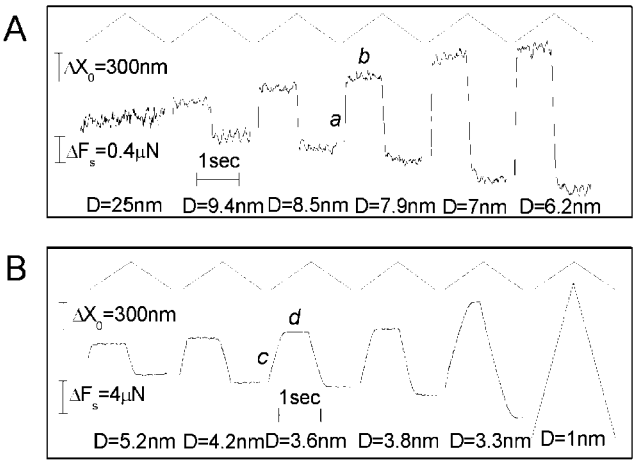

FIGURE 3. A and B: Shear forces between mica sheets bearing adsorbed PEO in PEO37/toluene solution, as the surfaces slide past each other, at different surface separations, D, as indicated. Each pair of traces monitors the uniform back-and-forth lateral displacement applied to the upper surface, as a function of time (top trace within each pair) together with the shear force transmitted to the lower surface (bottom trace within each pair). We show data collected at different contact positions from two different mica sheets. We present only one period of the shear response at each separation, but we note that each one of the responses repeated itself several times as long as D remained the same. In the *a* and *c* regimes there is both bending as well as sliding of the shear spring (see text). In the *b* and *d* regimes the surfaces are sliding freely past each other, while the magnitude of the forces in these regimes, which are due to bending of the shear springs (lower traces within each pair) represent the sliding or kinetic friction force. Scales of time, shear forces and lateral displacement, are indicated on the traces.

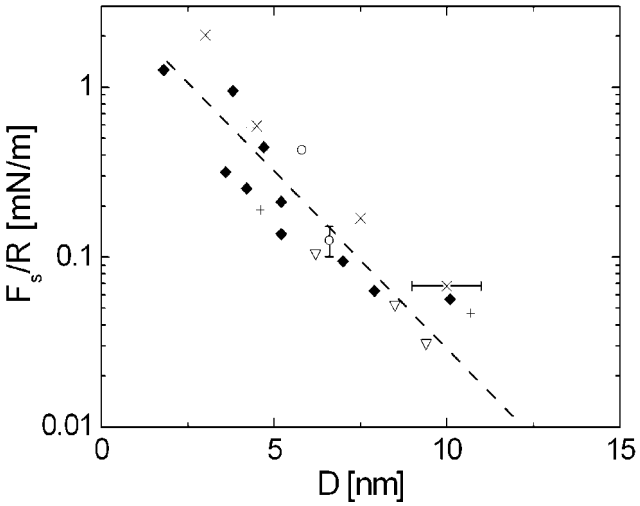

FIGURE 4. The variation of the shear forces $F_s(D)$ (normalized by R) between curved mica surfaces bearing adsorbed PEO in PEO/toluene solution, sliding past each other and taken from traces as in Fig. 3 (at sliding velocity v_s corresponding to that in Fig. 3), as a function of D. The magnitude of F_s shown is in all cases from the freely sliding region of each trace. Different symbols refer to different contact positions or experiments. The shear forces are below the detection limit for $D > 10$ nm.

frictional resistance, and steady sliding takes place (regions *b* and *d* in the traces): the magnitude of F_s in this plateau region at the different compressions is the kinetic friction force for this shear velocity.

At the higher compressions (Fig. 3B), the force increases strongly and monotonically, and the surface separations, D, become smaller than the closest approach attainable on normal compression alone. At the closest separations, $D = 1 \pm 0.5$ nm or so, the static frictional force exceeds the shear force and there is no sliding between the surfaces: they remain in rigid contact as the top surface moves laterally (right-hand trace in Fig. 3B). This approach almost to contact is an indication that at the highest compressions the PEO has been removed from the contact zone by shear, as directly confirmed by $F_n(D)$ profiles taken subsequent to the shear. In Fig. 4 the plateau values of F_s (the kinetic friction) are plotted against surface separation, based on traces as in Fig. 3. We find that F_s increases monotonically and exponentially with decreasing D.

As noted, the shear profiles were measured while approaching the surfaces following a compression run and separation. Because the shear itself changes the nature of the normal interactions (see below), the normal forces before shear serve as a reliable guide to the load, once shear measurements have been made, only for the regime of moderate compression (prior to the onset of large shear forces). We may define an effective kinetic friction coefficient $\mu_{eff} = F_s(D)/F_n(D)$. If we take the magnitude of F_n just at the onset of measurable F_s to be its value from the $F_n(D)$ profiles, and the magnitude of F_s at that point to be $\Delta F_s \approx 0.1$ μN at most, we find that at the onset point, $\mu_{eff} = 0.003$.

Normal Forces Following Shear

At the end of each of the shear runs (which lasted some 15 min from start to finish) the surfaces were taken apart. The surfaces were strongly adhered at the end of the shear run ($D \approx 0.5$–1 nm) and jumped out on separation to some 2–3 μm. To obtain further insight, we carried out a number of controls. $F_n(D)$ profiles taken immediately subsequent to the shear runs reveal the state of the adsorbed layers, and are shown in Fig. 5.

As clearly seen in Fig. 5, the $F_n(D)$ profile for is very different to its form prior to the shear: it shows a short-ranged repulsion (at $D < 3$ nm) on approach of the surfaces, and a marked attraction is observed on separating the surfaces following compression, when jump-outs occur–as shown in the inset. The magnitude of the attraction is greater than for bare mica surfaces in the toluene (Fig. 1), and we also note that it increases with the time of compression and to some extent with the magnitude of the compression itself (inset to Fig. 1). Comparison of the before-shear and after-shear $F_n(D)$ profiles, Fig. 2 versus Fig. 5, clearly shows that much of the PEO

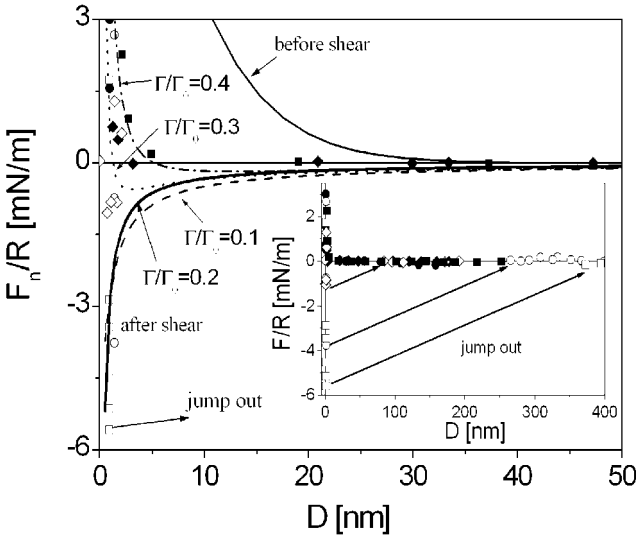

FIGURE 5. Normalized force–distance profiles (F_n/R) versus D following shear measurements between PEO-bearing mica surfaces. Measurements from different sets of experiments taken during compression and decompression of the two surfaces are shown. Different symbols refer to different contact positions on different mica sheets. Solid symbols indicate forces measured during compression and open symbols indicate forces measured during decompression. We indicate with the arrow (and show in the inset over a wider range of data) that on separation the surfaces jumped out to a far distance (zero force region). For comparison, normal force profiles, before shear, are presented as the top solid curve (based on the profiles in Fig. 2). The lower solid line is the force–distance profile calculated [38] for adsorbing PEO in water at 10% surface coverage and the dashed line is for 20% surface coverage (see text). The broken upper curves correspond to 30% and 40% surface coverage and fit the compression $F_n(D)$ profiles. *Inset*: The same force profiles with identical symbols, but here we included the range to which the surfaces jump out, when the pull-off force exceed the adhesion. At each of the force–distance profiles the maximum applied load under compression was different: the extent of the jump-out – proportional to the adhesive force – increased with increasing maximum load or load-time prior to pull-off.

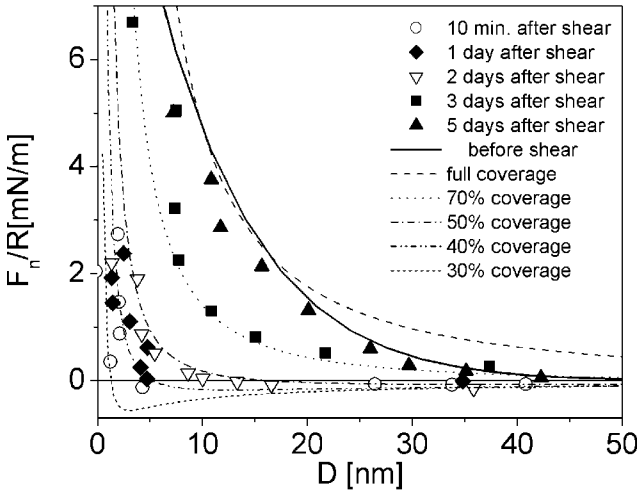

FIGURE 6. Normalized equilibrium force–distance profiles (F_n/R) versus D measured on compression, 10 min following shear measurements between PEO-bearing mica surfaces, and after incubation of 1 to 5 days in the PEO/toluene solution as indicated, while keeping a gap of 20 ± 5 μm between the surfaces. The broken curves are the corresponding force–distance profile calculated [38] for adsorbing PEO in water at 30% to 100% surface coverage. The equilibrium F_n/R before shear, referred as the 100% coverage, is indicated with the solid curve and is similar to that measured 5 days after shear.

has been removed from between the surfaces by the shear. The dependence of the adhesive strength on the compression time prior to separation further suggests that the adhesion is due to residual polymer chains bridging the gap, and that with time of compression more segments are forced onto the surfaces, resulting in stronger bridging. The solid and broken lower curves in Fig. 5 are the theoretically predicted bridging attractions–discussed in the following section–for interaction between surfaces bearing 10% and 20% of the equilibrium adsorbance of PEO in a good solvent. The broken upper curves which fit the compression force profiles, correspond to the theoretically predicted forces at 30% and 40%. Both the much-reduced separation for onset of repulsion on compression (2.5 ± 0.5 nm) and the marked bridging adhesion thus indicate that a substantial part of the PEO has been removed from the surfaces during the shear run.

Recovery of the Adsorbed Layer

The PEO solution was replaced with pure toluene (save for a meniscus between the surfaces), diluting it by factor of *ca.* 1000, and $F_n(D)$ profiles were determined to confirm equilibrium behaviour. Shear motion was then applied as before, following which normal force profiles were again measured. These were identical (within the scatter) to the $F_n(D)$ profiles taken after shear in the solution (Fig. 5). Then the surfaces were kept at a separation of *ca.* 20 ± 5 μm for two days to enable relaxation of chains on the surface. $F_n(D)$ profiles taken at various points during this period were similar to the $F_n(D)$ profiles measured immediately after shear. This sequence of measurements demonstrates directly that in the pure toluene, once the PEO chains had been removed by shear, there was little recovery of the adsorbed layer at the contact position, even after two days, suggesting that polymer from adjacent parts of the mica did not migrate along the mica to heal the sheared region.

The pure toluene was then replaced with the PEO solution, and the surfaces held at separation of 20 ± 5 μm for 5 days, to diffusion-limit the rate of arrival and adsorption of polymer at this region of interest (i.e., where $F_n(D)$ is measured) [36]. Normal force profiles measured at various times during this period are presented in Fig. 6 and show gradual recovery of the PEO adsorbed layer, clearly due to adsorption of new PEO chains from the solution.

The solid curve is the normal forces before shear and the broken curves in Fig. 6 are the theoretically predicted forces–discussed in the following section–for interaction between surfaces bearing 30% and up to full equilibrium adsorbance coverage of PEO in a good solvent.

DISCUSSION

The new finding in this paper concerns the recovery of the adsorbed layer in the contact region following the removal of PEO at high compressive loads by the shearing motion. The normal and shear forces have been analysed and discussed in detail elsewhere [25, 28–31; see also Raviv, Klein and Witten "The polymer mat: arrested rebound of a compressed polymer layer" (submitted)] the focus of this discussion is on the recovery of the adsorbed layers at the contact region, following shear, in a 20 ± 5 μm gap.

The amount of polymer adsorbed at equilibrium on the interacting surfaces, Γ_0, cannot be evaluated from refractive index measurements because the refractive index of PEO is very similar to that of toluene. However, it may be estimated from the force profiles to be $\Gamma_0 \approx 0.9 \pm 0.2\ \mathrm{mg/m^2}$, as was done in the earlier PEO/mica/toluene studies [25, 28]

The layer thickness at equilibrium $L \approx 4R_g$, suggesting that the chains are swollen. This, together with the clear evidence for the removal of the polymer chains by the shearing motion, indicates that the chains are weakly adsorbed to the mica surfaces (for PEO segments adsorbed onto mica from aqueous solution the net segment sticking energy in *ca.* 0.06 kT [37]). As a result, the lateral forces on the PEO chains are sufficient to desorb them from the adsorbing substrate so that under the strong compression they are squeezed out from between the region of closest approach. The final situation is one where the few PEO chains that remain on the surface are strongly bridging, resulting in the marked adhesion between the surfaces manifested in $F_n(D)$ profiles following shear (Fig. 5). An upper limit for the amount of polymer remaining following shear is obtained from the range of interactions on approach and compression, where the surfaces approach to separations of *ca.* 1 ± 0.5 nm at the highest compressions, indicating a maximal adsorbance of *ca.* $30 \pm 10\%$ of its value prior to shear.

We may try to estimate roughly the adsorbance remaining on the surfaces following shear and its increase with time by fitting to the prediction of a recent model [38] on interactions between surfaces bearing a sub-equilibrium adsorbance of chains in a good solvent. This model enables the forces between surface-adsorbed polymers in a good solvent to be calculated in terms of experimentally observable parameters, such as bulk osmotic pressures in the corresponding polymer solution, and the single surface segment-density profile (determined for example by neutron scattering). Using appropriate parameters (to calculate the curves in Figs 5 and 6 we used parameters corresponding to the water/PEO system taken from [38]) we generated the two lower attractive profiles in Fig. 5 corresponding to adsorbances of 10% and 20% of the equilibrium value, the two upper broken curves in Fig. 5 corresponding to adsorbance of 30% and 40% and the broken curves in Fig. 6 corresponding to adsorbance of 30–100%. The attraction for an adsorbance of 10–20% of its equlibrium value is basically due to bridging by the polymer dominating the interactions at low adsorbance. While these profiles do not describe the short-range repulsion on approach (filled data points in Fig. 5, which are described by the broken curve corresponding to absorbance of 30–40%, see also lower broken curves in Fig. 6), suggesting equilibrium bridging is not fully developed, they are roughly in the range of the adhesive forces on separation, once bridging has taken place following the compression.

The slow time for build-up of an adsorption layer in a narrow gap has been found and analysed for the case of adsorbed polymers in theta conditions [36]. It was found that the chains have to diffuse about 1–2 mm in the narrow 20–100 μm gap created between the mica surfaces to reach the region of closest approach. The characteristic time τ for the surfaces at the region of closest approach to attain the limiting full adsorbance was estimated to be of order 5×10^5 sec (some days) in conditions very similar to our experiments. This supports our finding of slow recovery of adsorbed layer and indicates that the recovery is diffusion-limited.

Finally we note that higher M_w PEO behaves in a different way [25]. This is because its total adsorption is stronger and its surface layer is more entangled, and therefore it is less likely to desorb by the applied lateral force.

CONCLUSIONS

We have shown that the adsorbed PEO chains of $M_w = 37$ kg/mol adsorb weakly on mica surfaces from PEO/toluene solution and that the lateral force applied in the SFB under strong compression is enough to desorb $80 \pm 10\%$ of the chains from the contact region. The remaining chains can bridge between the two surfaces when they are close enough. We studied the recovery of adsorbed polymer layers in a narrow gap and dilute solution. Our results reveal that no migration occurs on the surface and that the adsorbed layers recover within a few days only by adsorption of polymers that diffuse slowly into the narrow gap.

ACKNOWLEDGEMENTS

We thank the Eshkol Foundation for a studentship to U.R. The support of the US-IL Binational Science Foundation and the German-Israel Foundation (GIF) is acknowledged with thanks.

REFERENCES

1. Fleer GJ, Cohen-Stuart MA, Scheutjens JMHM, Cosgrove T, Vincent B. *Polymers at Interfaces*. Chapman & Hall: London, 1993.
2. Napper DH. *Polymeric Stabilization of Colloidal Dispersions*. Academic Press: London, 1983.
3. Lee LH. *Fundamentals of Adhesion*. Plenum: New York, 1991.
4. Leger L, Joanny JF. Liquid spreading. *Rep. Prog. Phys.* 1992; **55**(4): 431–486.
5. Yerushalmi-Rozen R, Klein J. Stabilisation of thin non-wetting liquid films on a solid substrate by polymeric additives. *Langmuir* 1995; **11**: 2806.
6. Yerushalmi-Rozen R, Klein J, Fetters LJ. Brush stabilisation of thin films. *Science* 1994; **263**: 793.
7. Belfort G. Membrane fouling. *Langmuir* 1997; in press.
8. Sung LK, Morris KE, Taylor JS. Predicting colloidal fouling. *Desalination and Water Reuse* 1994; **38**.
9. Luckham PF. Recent advances in polymers at surfaces: the steric effect. *Colloid & Interface Science* 1996; **1**: 39–47.
10. Eiser E, Klein J, Witten TA, Fetters LJ. Shear of telechelic brushes. *Phys. Rev. Lett.* 1999; **82**(25): 5076–5079.
11. Leckband DE, Israelachvilli JN, Schmitt FJ, Knoll W. Rearrangement in receptor ligand interactions. *Science* 1992; **255**: 1419–1421.
12. Patel S, Tirrell M. Steric forces between polymer-bearing surfaces. *Ann. Rev. Phys. Chem.* 1989; **40**: 597–624.
13. Raviv U, Laurat P, Klein J. Fluidity of water confined to sub-nanometre films. *Nature* 2001; **413**: 51–54.
14. Janik J, Tadmor R, Klein J. Shear of molecularly confined liquid crystals. 1. Orientation and transitions under confinement. *Langmuir* 1997; **13**: 4466–4473.
15. Klein J, Perahia D, Warburg S. Forces between polymer-bearing surfaces undergoing shear. *Nature* 1991; **352**: 143–145.
16. Klein J, Kamiyama Y, Yoshizawa H, Israelachvilli JN, Fredrickson GH, Pincus P, Fetters LJ. Lubrication forces between surfaces bearing polymer brushes. *Macromolecules* 1993; **26**(21): 5552–5560.
17. Klein J. Shear of polymer brushes. *Colloids and Surfaces A* 1994; **86**: 63–76.
18. Klein J, Kumacheva E, Perahia D, Mahalu D, Warburg S. Interfacial sliding of polymer-bearing surfaces. *Faraday Discuss.* 1994; **98**: 173–188.
19. Klein J, Kumacheva E, Mahalu D, Perahia D, Fetters L. Reduction of frictional forces between solid surfaces bearing polymer brushes. *Nature* 1994; **370**: 634–636.
20. Klein J. Shear, friction, and lubrication forces between polymer-bearing surfaces. *Ann. Rev. Mater. Sci.* 1996; **26**: 581–612.
21. Klein J, Kumacheva E, Perahia D, Fetters LJ. Shear forces between sliding surfaces coated with polymer brushes: the high friction regime. *Acta Polym.* 1998; **49**: 617–625.
22. Kumacheva E, Klein J. Simple liquids confined to molecularly thin layers. II. Shear and frictional behavior of solidified films. *J. Chem. Phys.* 1998; **108**(16): 7010–7022.
23. Neelov IM, Borisov OV, Binder K. Shear deformation of two interpenetrating polymer brushes: stochastic dynamics simulation. *J. Chem. Phys.* 1998; **108**: 6973–6988.
24. Qian L, Luengo G, Douillet D, Charlot M, Dollat X. New two-dimensional friction force apparatus design for measuring shear forces at the nanometer scale. *Rev. Sci. Instruments* 2001; **72**(11): 4171–4177.
25. Raviv U, Tadmor R, Klein J. Shear and frictional interactions between adsorbed polymer layers is a good solvent. *J. Phys. Chem. B* 2001; **105**: 8125–8134.
26. Harris JM. *Poly(ethylene glycol) Chemistry: Biotechnical and Biomedical Application*. Plenum Press: New York, 1992.
27. Bailey FE, Jr, Koleske JV. *Poly(ethylene glycol)*. Academic Press: New York, 1976.
28. Luckham PF, Klein J. Interactions between smooth solid surfaces in solutions of adsorbing and non-adsorbing polymers in good solvent conditions. *Macromolecules* 1985; **18**(4): 721–728.
29. Klein J, Luckham PF. Long-ranged attractive forces between two mica surfaces in an aqueous polymer solution. *Nature* 1984; **308**(26): 836–837.
30. Klein J, Luckham PF. Forces between two adsorbed poly(ethylene oxide) layers in a good aqueous solvent in the range 0–150 nm. *Macromolecules* 1984; **17**(5): 1041–1048.
31. Luckham PF, Klein J. Forces between mica surfaces bearing adsorbed homopolymers in good solvent: the effect of bridging and dangling tails. *J. Chem. Soc. Faraday Trans.* 1990; **86**(9): 1363–1368.
32. Klein J. Forces between mica surfaces bearing adsorbed macromolecules in liquid media. *J. Chem. Soc. Faraday Trans.* 1983; **79**: 99–118.
33. Klein J, Kumacheva E. Simple liquids confined to molecularly thin layers. I. Confinement-induced liquid to solid phase transitions. *J. Chem. Phys.* 1998; **108**(16): 6996–7009.
34. Derjaguin BV, Churaev NV, Muller VM. *Surface Forces*. Plenum Publishing: New York, 1987.
35. Christenson HK. Structural forces. *J. Chem. Phys.* 1983; **78**: 6906–6913.
36. Almog Y, Klein J. Interactions between mica surfaces in polystyrene-cyclopentane solution near the θ-temperature. *J. Colloids Interface Sci.* 1985; **106**(1): 33–44.
37. Raviv U, Frey J, Sak R, Laurat P, Tadmor R, Klein J. *Langmuir* in press.
38. Klein J, Rossi G. Analysis of the experimental implications of the scaling theory of polymer adsorption. *Macromolecules* 1998; **31**(6): 1979–1988.
39. Derjaguin BV. *Kolloid Zh.* 1934; **69**: 155–164.